Heliyon 10 (2024) e38221

Contents lists available at ScienceDirect

Heliyon

journal homepage: www.cell.com/heliyon

Research article

Survival prediction and analysis of drug-resistance genes in HER2-positive breast cancer

Lin Yang [***,1], Songhao Chen [1], Meixue Wang, Shujia Peng, Huadong Zhao, Ping Yang, Guoqiang Bao [**], Xianli He [*]

Department of General Surgery, The Second Affiliated Hospital of Air Force Medical University, Xi'an, 710038, Shaanxi, China

ARTICLE INFO

Keywords:
Drug resistance
HER2-Positive breast cancer
Risk signature
eccDNA
Non-coding RNA
MED1

ABSTRACT

Despite the approval of several therapeutic agents for HER2-positive breast cancer, drug resistance remains a significant challenge, hindering the patient's prognosis. Thus, our study aimed to establish a risk model to predict the prognosis of patients and identify key genes regulating drug resistance in HER2-positive breast cancer. Utilizing data from The Cancer Genome Atlas (TCGA) and Gene Expression Omnibus (GEO), a predictive model was constructed based on 5 drug resistance-related genes, which demonstrated a notable capacity to indicate the survival rates of patients. Besides, through eccDNA and transcriptome sequencing of drug-sensitive and resistant cancer cells, 3 significant DEGs were identified: MED1, MED24, and NMD3. Among them, MED1 showed the most significant elevation in drug-resistance cells, highlighting its crucial role in mediating drug resistance. MED1 may serve as a valuable target for alleviating drug resistance in HER2-positive breast cancer.

1. Introduction

Breast cancer, the most frequently diagnosed cancer worldwide, is a primary cause of mortality among women [1]. Human epidermal growth factor receptor 2 (HER2) is a member of the epidermal growth factor receptor (EGFR) family with intrinsic tyrosine kinase function, which is abnormally overexpressed in approximately 15–20 % of breast cancer cases [2,3]. Despite continuous improvements in oncologic outcomes, drug resistance may also develop and cause a considerable fraction of patients with advanced HER2-positive breast cancer to succumb to the disease, which can severely reduce chemotherapy effectiveness and lead to poor prognosis [4,5]. Thus, it is critical to investigate the molecular mechanisms underlying therapeutic resistance for developing more effective therapies and improving the patient's prognosis.

Previous studies have pointed out that the ErbB family, including ErbB1, ErbB2, ErbB3, and ErbB4 [also known as EGFR (HER1), HER2, HER3, and HER4, respectively], plays a vital role in cell differentiation, proliferation, migration, and survival [6,7]. Alterations in ErbB family genes are tightly implicated in cancer development, which can drive tumorigenesis and dampen anti-tumor immune

* Corresponding author. Department of General Surgery, The Second Affiliated Hospital of Air Force Medical University, Xi'an, 710038, Shaanxi, China.
** Corresponding author.
*** Corresponding author.
E-mail addresses: Peteryang828@126.com (L. Yang), guoqiangfmmu@163.com (G. Bao), hexltd@163.com (X. He).
[1] They contributed equally to this paper.

https://doi.org/10.1016/j.heliyon.2024.e38221
Received 22 January 2024; Received in revised form 18 September 2024; Accepted 19 September 2024
Available online 20 September 2024

responses [8,9]. It has been demonstrated that upregulation of EGFR is a key mechanism of resistance in breast cancer cells, which participates in maintaining stem-like tumor cells and promoting bone metastasis [10–12]. Additionally, overexpressed HER2 has been frequently found in a significant proportion of breast cancer patients, which is closely associated with treatment resistance and the subsequent poor clinical prognosis [13,14]. Recent findings have highlighted that CMTM6 inhibits HER2 ubiquitination, stabilizing HER2 protein and contributing to trastuzumab resistance in HER2-positive breast cancer cells [15]. In particular, the ER-IGF1R-ErbB signaling, activated by RBP2, is highly correlated with a poor prognosis to tamoxifen therapy in ER-positive breast cancer as it induces tamoxifen resistance [16]. Additionally, activation of the ErbB/PI3K/Akt signaling pathway boosted by lncRNA PCAT7 has been evidenced to potentiate breast cancer cell proliferation, migration, and invasion while suppressing cell apoptosis [17]. Thus, targeting the ErbB signaling pathway and related genes may lead to new therapies addressing drug resistance and improving the prognosis of breast cancer patients.

In this study, gene expression data and clinical information concerning breast cancer samples were downloaded from The Cancer Genome Atlas (TCGA) database and the HER2-positive breast cancer-related GSE89216 dataset (containing drug-resistant and drug-sensitive samples) from the Gene Expression Omnibus (GEO) database. Key genes associated with the ErbB signaling pathway were identified using various computational biology methods, and a gene signature was constructed to predict disease prognosis as well as screen the crucial genes involved in drug resistance in HER2-positive breast cancer patients.

2. Materials and methods

2.1. Clinical data analysis

The clinical data from 359 patients with HER2-positive breast cancer were collected. Patients were allocated into 3 groups based on the targeted therapy they received: no targeted therapy, single targeted drug therapy, and dual targeted therapy. Then, the number and proportion of patients with pathologic complete response (pCR) in different groups were analyzed, as well as the occurrence of tumor recurrence or metastasis during follow-ups. All patients signed the informed consent forms. The Chi-square test or Fisher's exact test was used for the analysis of intergroup differences, considering $p < 0.05$ as statistically significant. Statistical analysis was performed using SPSS 26.0 software.

2.2. Data collection

Raw sequencing data of HER2-positive breast cancer patients were downloaded from the TCGA database (https://portal.gdc.cancer.gov/), including expression data and clinical information of a total of 1113 tumor samples and 113 matched normal samples of breast cancer [18]. Besides, based on the clinical information, a subset of 164 samples with positive HER2 status (lab_proc_her2_neu_immunohistochemistry_receptor_status) was selected for prognosis analysis. Raw sequencing data were obtained from the TCGA dataset, and access to this data was controlled by the TCGA project team. The relevant expression files and clinical information were acquired through the TCGA data portal following all necessary access permissions and ethical guidelines. The study was conducted in compliance with the TCGA data usage policy.

For drug resistance analysis, the HER2-positive breast cancer dataset GSE89216 (Last update: Jan 01, 2020) from the GEO database was retrieved, consisting of 4 resistant (Resistant) samples and 4 drug-sensitive (Sensitive) samples [19].

2.3. Identification of genes associated with the ErbB signaling pathway

A total of 85 constituent genes of the ErbB signaling pathway were obtained from the Kyoto Encyclopedia of Genes and Genomes (KEGG) database [20], as the ErbB signaling pathway (hsa04012) is critical for HER2 regulation and drug resistance in breast cancers.

2.4. Identification of a risk signature associated with HER2-positive breast cancer

Genes co-expressed with the ErbB signaling pathway ($|cor| > 0.7$ and $p < 0.05$) were identified through Pearson correlation analysis. After that, prognosis-related genes in HER2-positive patients were identified using the univariate Cox regression analysis with a threshold of $p < 0.05$. LASSO Cox regression analysis identified genes affecting overall survival (OS) using the variable selection and shrinkage in the R package "glmnet". The independent variables in the regression were the normalized expression matrix of candidate prognostic genes, while the response variables were the total survival time as well as the status of patients from the TCGA cohort. The penalty parameter (λ) was determined through tenfold cross-validation following the minimum criterion (i.e., λ value corresponding to the lowest partial likelihood deviance). Furthermore, the regression coefficients (β) obtained from the LASSO Cox regression model were combined with mRNA expression levels to construct a prognostic gene signature by calculating a risk score using the following formula:

Risk score = (βmRNA1 * mRNA1 expression level) + (βmRNA2 * mRNA2 expression level) + (βmRNA3 * mRNA3 expression level) + … + (βmRNAn * mRNAn expression level).

Based on the median risk score, patients were then allocated into the high-risk and low-risk groups. Time-dependent receiver operating characteristic (ROC) curves were generated to assess the predictive value of the prognostic gene signature for the OS. Furthermore, the differences in survival between the high-risk and low-risk groups were compared using Kaplan-Meier survival curves and the Log-rank test.

2.5. Identification of differentially expressed genes (DEGs)

Extrachromosomal circular DNA (eccDNA) and whole transcriptome sequencing (including mRNA and other non-coding RNA) were performed on the HER2-positive breast cancer cell line SK-BR-3 and drug-resistant cell JIMT-1. Next, differential analysis on transcriptome sequencing data (mRNA) of SK-BR-3 cells and JIMT-1 cells was performed using the R package "DESeq2". With a threshold for DEGs of $|\log2(\text{fold change})| \geq 0.5$ and p-value <0.05, a total of 745 DEGs were obtained, including 364 upregulated and 381 downregulated genes. A heatmap of these DEGs was generated based on the analysis results.

2.6. Function and pathway enrichment analysis

Gene Ontology (GO) terms and KEGG pathway enrichment analyses were performed using the R package "clusterProfiler" on HER2-regulating associated genes, as well as the differentially expressed circular DNA with a significance threshold of p-value <0.05 [21].

Classical signaling pathway enrichment analysis of DEGs was also performed using the IPA software [22]. Pathways with a significance threshold of $p < 0.05$ were selected and then ranked based on -log(P) value. A positive Z-score (>0) indicated pathway activation, while a negative Z-score (<-0) indicated pathway inhibition.

2.7. Establishment of protein-protein interaction (PPI) networks

Protein interaction relationships with differential eccDNA were obtained using the STRING database (https://string-db.org/), a resource that can provide known and predicted protein-protein interactions [23]. The PPI analysis of differential eccDNA genes was performed using Cytoscape software [24].

2.8. Real-Time quantitative polymerase chain reaction (RT-qPCR)

The total RNA of the cultured SK-BR-3 and JIMT-1 cells was extracted using the TRIzol reagent and then reverse-transcribed into cDNA using the SureScript-First-strand-cDNA-synthesis-kit (Servicebio) as per the manufacturer's instructions. Real-time qPCR was performed in a CFX96 Real-Time PCR Detection System (Bio-Rad), and the data were analyzed using the $2^{-\triangle\triangle Ct}$ method [25]. The primers used in this manuscript were:

MED1-F: CAAAGCGGAAGAAGGCAGAC; MED1-R: GGAAGAATGGCTATGGTGGC; MED24-F: GTGCTGTGGCTTGGCTTGT; MED24-R: CGGTGGAGGGAAACTTGAT; NMD3-F: TGGTGTTAGGGTTTGATTTGGC: NMD3-R: TTCTACGACGCTGACGTTTGGT; GAPDH-F: CGAAGGTGGAGTCAACGGATTT; GAPDH-R: ATGGGTGGAATCATATTGGAAC.

2.9. Cell line culture

SK-BR-3 and JIMT-1 cells were cultured in DMEM (Gibco) supplemented with 10 % fetal bovine serum (FBS) and 1 % penicillin/streptomycin in a humidified incubator (37 °C, 5 % CO_2).

2.10. Sequencing library construction

For eccDNA sequencing, DNA was extracted using the QIAamp DNA Mini Kit (Qiagen). Circular DNA was enriched using the Plasmid-Safe ATP-Dependent DNase (Epicentre), followed by library construction using the NEBNext Ultra II DNA Library Prep Kit (New England Biolabs). For whole transcriptome sequencing, total RNA was extracted using the TRIzol reagent (Invitrogen). RNA-seq libraries were prepared using the NEBNext Ultra RNA Library Prep Kit for Illumina (New England Biolabs) following the manufacturer's protocols.

2.11. Data preprocessing

For RNA-seq data, quality control was performed using FastQC, and low-quality reads were trimmed using Trimmomatic. Reads were aligned to the human reference genome (hg38) using HISAT2, and gene expression quantification was performed using featureCounts.

2.12. Cell count kit-8 (CCK-8) assays

Cells with SKBR3 overexpression were utilized for CCK-8 assay. In short, cells at the log phase were digested with trypsin and prepared into a $1 \times 10\hat{}5$ cells/mL suspension. Next, cells were seeded (1×10^4 cells/well) in 96-well plates and incubated (37 °C, 5 % CO_2) until adherence. Then, the medium was replaced with serum-free medium [containing 1 % bovine serum albumin (BSA)] for 12 h. Subsequently, cells were treated with trastuzumab at concentrations of 1 μg/mL and 10 μg/mL, with cells in the control groups receiving the solvent medium and blank wells containing medium only. After 24 h, the medium was replaced with 100 μL of CCK-8 working solution, followed by incubation for 1–4 h. The absorbance at 450 nm was measured using a microplate reader. Cell viability was calculated as follows: Proliferation Rate (%) = (Experiment - Blank)/(Control - Blank) × 100 %.

2.13. Western blot

Total protein was extracted from adherent cells by PBS washing, lysed in protein extraction reagent supplemented with protease inhibitors, and incubated on ice. Lysates were centrifuged, with the supernatant collected for protein concentration determination

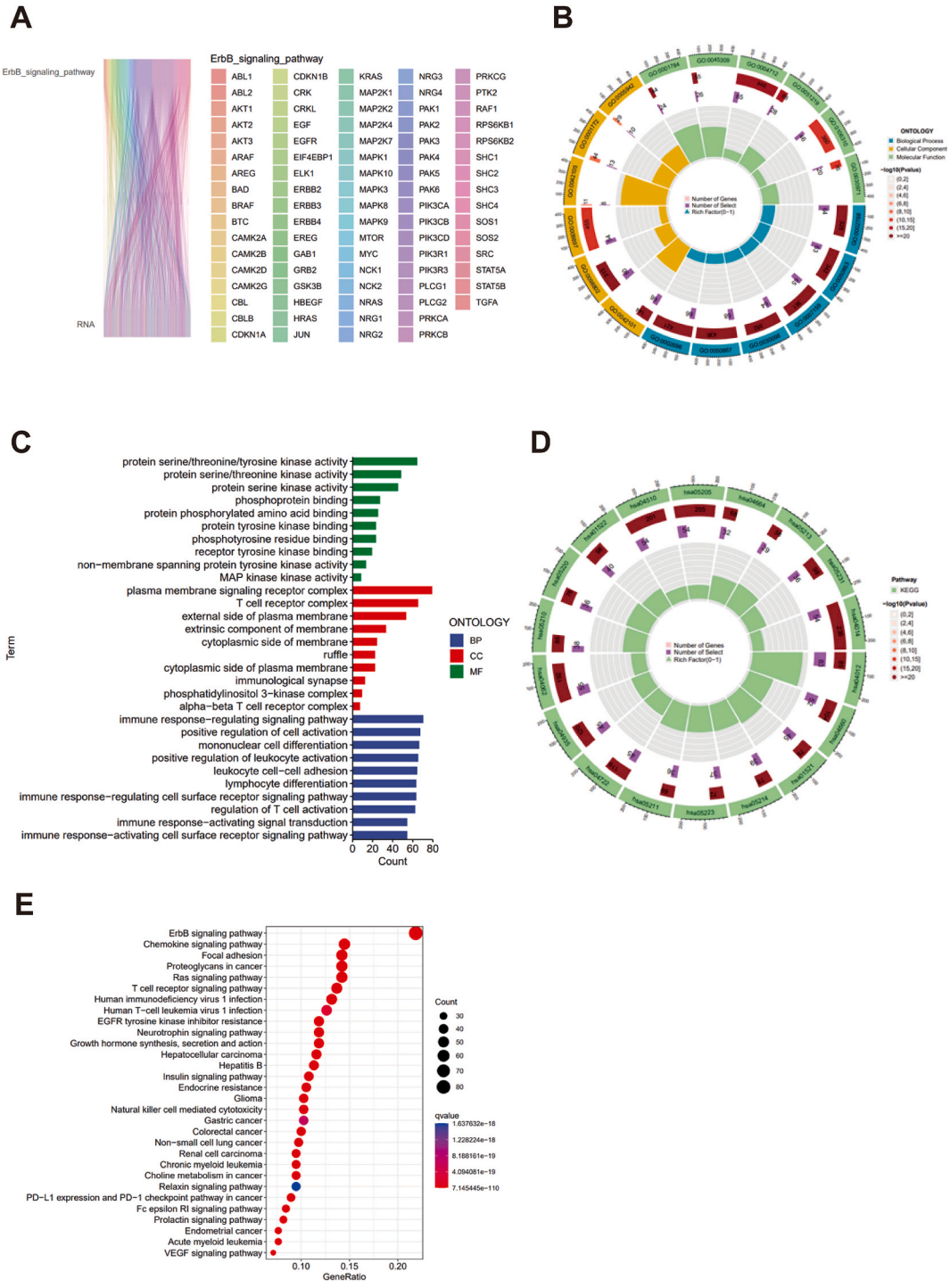

Fig. 1. Functional analysis of ErbB pathway-associated genes. (A) The co-expression analysis of ErbB pathway-related genes with RNAs of HER2-positive breast cancer patients. (B) The circular plot of GO analysis. (C) The bar chart of the GO analysis. (D) The circular plot of KEGG analysis. (E) The bar chart of the KEGG analysis.

using a bicinchoninic acid (BCA) assay kit. After denaturation, protein samples (40 μg each) were subjected to sodium dodecyl sulfate-polyacrylamide gel electrophoresis (SDS-PAGE) and then transferred to PVDF membranes. The membranes were blocked and then incubated (overnight, 4 °C) with primary antibodies, followed by washing with TBST. After that, the membranes were incubated with HRP-conjugated secondary antibodies and finally subjected to chemiluminescent detection using electrochemiluminescence (ECL) solution.

2.14. Xenograft tumor formation assay

For the xenograft tumor formation assay, JIMT-1 cells with MED1 knockdown and control cells, as well as SKBR3 cells with MED1 overexpression and their respective controls, were used. Cells at the logarithmic growth phase were harvested, washed, and resuspended in PBS. Nude mice (4–6 weeks old) were subcutaneously injected with $1 \times 10\hat{}6$ cells in a total volume of 100 μL per site. Tumor growth was monitored bi-weekly using calipers, and tumor volumes were calculated using the following formula: volume = (length × width^2)/2. At the end of the study period, mice were sacrificed, and their tumors were excised, weighed, and analyzed. All animal procedures were approved by the Institutional Animal Care and Use Committee.

2.15. Statistical analysis

The relationship between prognosis gene expression levels and clinically qualitative variables (including gender, age, tumor stage, and TNM stage) were compared using the Chi-square test and Fisher's exact test. Genes associated with the ErbB signaling pathway were screened using Pearson correlation analysis. T-test was used for examining paired samples while the non-parametric Wilcoxon rank-sum test was used for unpaired samples. The OS between different groups was compared using Kaplan-Meier analysis with a Log-rank test. Independent predictors of the OS were determined utilizing the univariate and multivariate Cox regression analysis. All statistical analyses were performed using R software (version 4.2.1) [26]. Unless specified above, $p < 0.05$ is considered statistically significant.

3. Results

3.1. Analysis of the efficacy of targeted therapy

For reflecting the effectiveness of targeted therapy in HER2-positive breast cancer patients, the pCR of patients who received the neoadjuvant chemotherapy (including Trastuzumab, Pertuzumab, or a combination of them) was analyzed. The results showed that only about 22 % of patients who received targeted therapy demonstrated pCR. Moreover, among them, patients with the combined use of Trastuzumab and Pertuzumab earned the best efficacy, compared to those with no targeted therapy or only a single type of therapy (Supplementary Table 1). Besides, we found that patients who received targeted therapy were more prone to tumor metastasis compared to those with no targeted therapy (Supplementary Table 2). This indicated that tumor cells with developed drug resistance could possess a more aggressive phenotype compared to primary tumor cells. All these data showed that the drug resistance of HER2-positive cancers remained a significant barrier to cancer patient's survival.

3.2. Analysis of ErbB pathway-associated genes

Since the ErbB pathway is a critical regulator of HER2 signaling transduction in breast cancer, and the ErbB pathway was also found highly related to the achievement of drug resistance in HER2-positive breast cancers, we aimed to identify key genes regulating the ErbB signaling pathway in HER2-positive breast cancer patients. Thus, a co-expression correlation analysis was first performed. RNA sequencing data of HER2-positive breast cancer patients were obtained from the TCGA database and the list of 85 genes involved in the ErbB signaling pathway (hsa04012) was identified from the KEGG database. RNA sequencing data were normalized using the Transcripts Per Million (TPM) method and log2 transformation was applied. A pairwise co-expression analysis was performed between the 85 ErbB pathway genes and the entire RNA profile of HER2-positive breast cancer patients; the Pearson correlation coefficients (PCC) for each gene pair were calculated to measure the strength and direction of their linear relationship. With a threshold of $|cor| > 0.7$ and $p < 0.05$, a total of 1001 genes were identified as significantly correlated with the ErbB signaling pathway in HER2-positive breast cancer patients. These genes were visualized in a correlation network (Fig. 1A). Subsequently, GO and KEGG enrichment analyses were performed to investigate the functions of these 1001 genes correlated with the regulation of HER2. As shown by the results, regarding cellular components (CC), the HER2-regulating genes were significantly enriched in T-cell receptors, including the T-cell receptor complex and alpha-beta T-cell receptor complex. Besides, the biological processes (BP) enrichment analysis revealed a relationship to immune responses, such as immune response-regulating cell surface receptor signaling pathway, regulation of T-cell activation, leukocyte cell-cell adhesion, and lymphocyte differentiation, while the molecular functions (MF) of these genes were associated with amino acid binding processes, including phosphotyrosine residue binding, protein phosphorylated amino acid binding, and protein serine/threonine/tyrosine kinase activity (Fig. 1B and C). Additionally, the KEGG analysis results demonstrated that these genes were significantly enriched in pathways related to tumor formation (Proteoglycans in cancer), drug resistance (EGFR tyrosine kinase inhibitor resistance), and immune responses (T cell receptor signaling pathway) (Fig. 1D and E).

3.3. Construction of a predictive model based on ErbB signaling pathway-related genes

Furthermore, a single-factor Cox regression analysis of the 1001 HER2 regulation-associated genes was performed and 261 prognostic-related genes were identified ($p < 0.05$). After that, the LASSO regression analysis was conducted on these 261 genes using iterative analysis with cross-validation. It was found that when the variable number was 12, the model had the lowest root mean square error (Fig. 2A). Subsequently, multi-factor Cox stepwise regression analysis was performed on the 12 genes, and a final multi-factor regression model for HER2-positive patients was obtained, which consisted of 5 genes (TRAV8-3, TMEM161A, OPA1, HRAS, and GP1BA) (Fig. 2B). Among them, TRAV8-3, TMEM161A, OPA1, and HRAS were identified as independent factors for predicting HER2-positive patients ($p < 0.05$). The risk score for this model was examined according to the following formula: risk score = (−0.454) * expression of TRAV8-3 + (0.061) * expression of TMEM161A + (0.060) * expression of OPA1 + (−0.026) * expression of HRAS + (−0.616) * expression of GP1BA. Moreover, time-dependent ROC analysis was also utilized on the predictive model with 5 above-mentioned genes in HER2-positive breast cancer patients. The results showed that this model had excellent predictive performance

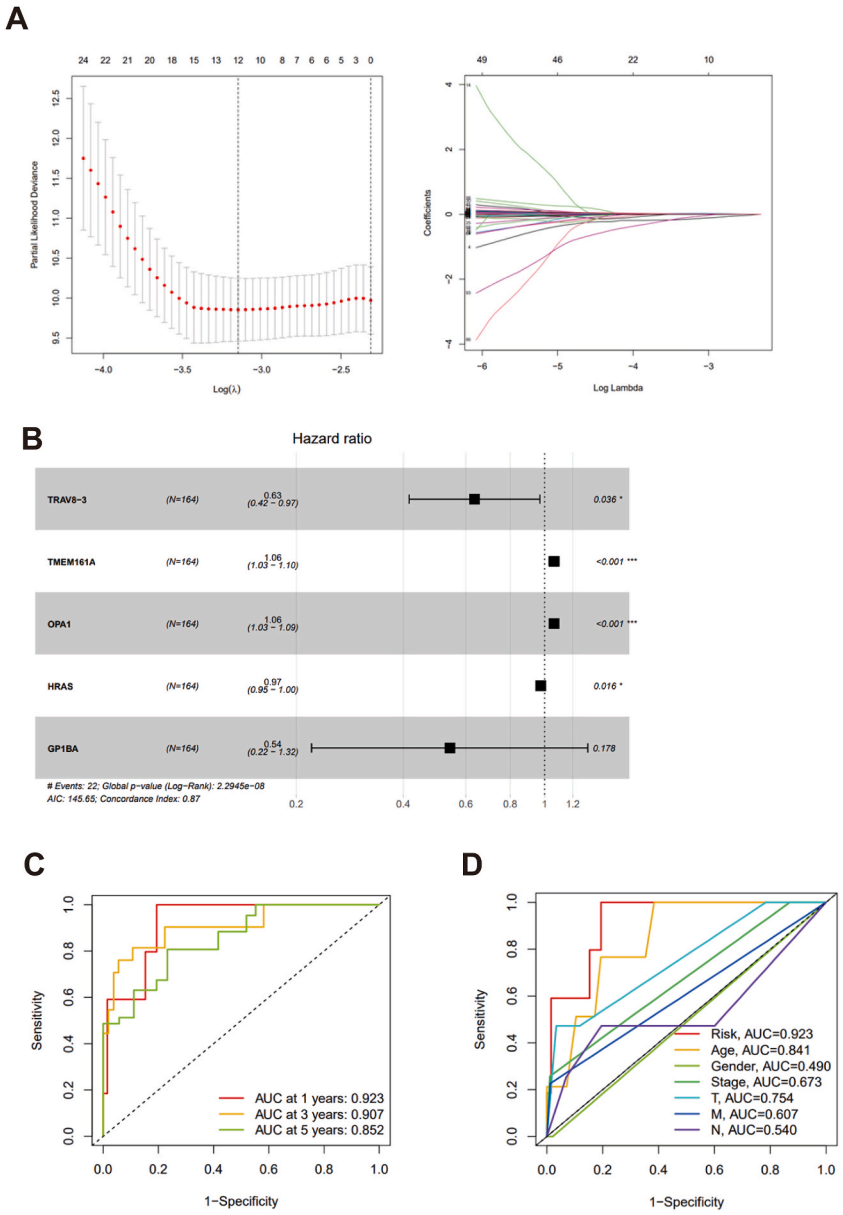

Fig. 2. Establishment of a predictive model for prognosis. (A) The LASSO regression analysis on 261 HER2-regulating prognostic genes. (B) Forest plot of the multifactor regression model. (C) The ROC curve for 1-year, 3-year, and 5-year survival rates of the 5-gene-based risk model. (D) The ROC curve comparing the 5-gene prognostic model with clinical factors.

for the prognosis of HER2-positive breast cancer patients, with the AUC values of 0.923, 0.907, and 0.852 for 1-year, 3-year, and 5-year survival rates, respectively (Fig. 2C). Additionally, the prediction ability of this model for 1-year survival rate (AUC: 0.923) was significantly better than other indicators, such as age (AUC: 0.841) (Fig. 2D).

3.4. Kaplan-Meier survival analysis

The above results indicated that this 5-gene model could serve as a promising candidate for predicting the survival rates of HER2-positive breast cancer patients. Therefore, HER2-positive breast cancer patients were allocated into the high-risk and low-risk two groups, with the median risk score of the prognostic model as a cutoff value. Additionally, as indicated by the Kaplan-Meier survival analysis results, the low-risk group showed a significantly higher survival rate than the high-risk group (Log-rank test: $p < 0.001$) (Fig. 3A). Furthermore, Kaplan-Meier survival analysis was performed on the 5 genes (TRAV8-3, TMEM161A, OPA1, HRAS, and GP1BA), stratifying patients into the high-expression and low-expression groups based on the median expression level. The results revealed that patients with high expression levels of TMEM161A and OPA1 showed notably lower survival rates (Log-rank test: $p < 0.001$) (Fig. 3B), while patients with high expression levels of TRAV8-3, HRAS, and GP1BA exhibited significantly higher survival rates (Log-rank test: $p < 0.001$) (Fig. 3C).

Besides, for validating whether the five-gene predictive model was an independent prognostic factor apart from other clinical variables, single-factor, and multi-factor Cox analyses were conducted on the model's risk scores and clinical factors. The single-factor Cox analysis results indicated that age, tumor stage, T stage, and the prognostic risk model were all risk factors for the prognosis of HER2-positive breast cancer patients, which were notably associated with the OS (HR > 1, $p < 0.05$) (Fig. 3D). Moreover, the multi-factor Cox analysis results revealed that age, tumor stage, T stage, N stage, and the 5-gene risk model were independent prognostic factors for HER2-positive breast cancer patients (HR > 1, $p < 0.05$) (Fig. 3E).

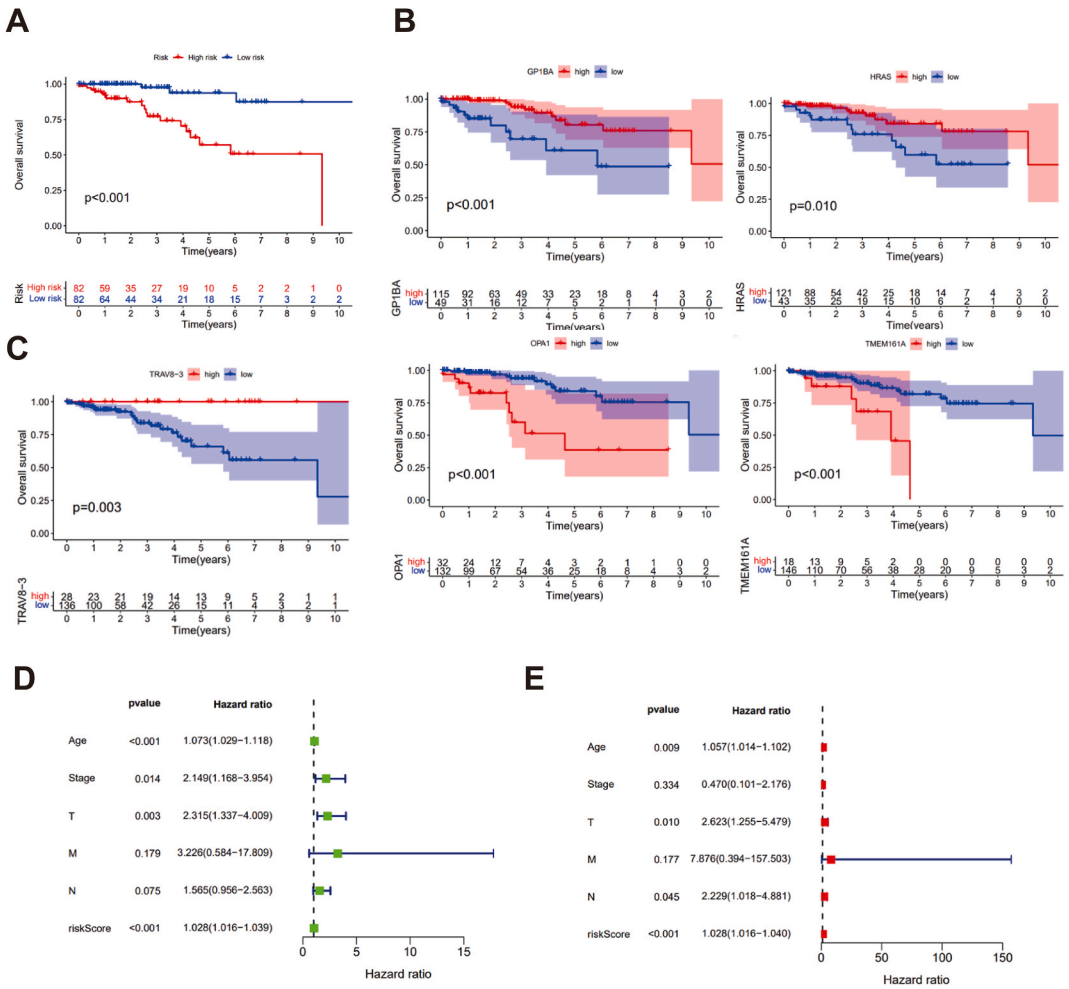

Fig. 3. Kaplan-Meier survival analysis based on predictive model. (A) The survival curve based on the 5-gene prognostic model. (B) The single gene survival curves for the constructed risk model. (C) Single-factor analysis of factors influencing the survival rates of HER2-positive patients. (D) Multi-factor Cox analysis of factors influencing the survival rates of HER2-positive patients.

3.5. The correlation between the ErbB signaling pathway-related predictive model and clinical factors

Furthermore, the correlation between the established risk model with clinical factors was investigated. With the median expression level of these 5 genes (TRAV8-3, TMEM161A, OPA1, HRAS, and GP1BA) from the prognostic model as the cutoff values, the relationship between single-gene differential expression and clinical factors (such as age, gender, tumor stage, and TNM stage) was compared. The results showed that TRAV8-3 expression was significantly associated with the age of HER2-positive breast cancer patients ($p < 0.05$) (Fig. 4A). TMEM161A expression had no significant correlation with all 6 clinical factors ($p > 0.05$) (Fig. 4B). OPA1 expression was remarkably associated with the N stage of patients ($p < 0.05$) (Fig. 4C), while HRAS expression was significantly associated with the T stage of patients ($p < 0.05$) (Fig. 4D). Additionally, GP1BA expression was noticeably associated with the age of patients ($p < 0.05$) (Fig. 4E).

3.6. Identification and functional analysis of drug resistance-related genes

Genes related to drug resistance of HER2-positive breast cancer were further validated. Through the dataset, GSE89216 from the GEO database, comprising 4 resistant (Resistant) samples and 4 drug-sensitive (Sensitive) samples, the DEGs between the two types of samples were then analyzed, and 70 upregulated genes and 77 downregulated genes were identified in the Resistant samples compared to the Sensitive samples (Fig. 5A and B). Additionally, considering that the eccDNA is the circular DNA molecules that exist outside of the chromosomes in a cell forming through genomic instability and chromothripsis, which is now believed to play an important role in regulating cancer cell drug resistance [1], it was also investigated. Thus, the (eccDNA) and transcriptome sequencing was performed with the HER2-positive breast cancer cell line (SK-BR-3) and the drug-resistant cell line (JIMT-1) (Supplementary Fig. 1A-1E). Differently expressed mRNA were first analyzed, and 364 upregulated genes and 381 downregulated genes were identified (Fig. 5C and D). Furthermore, DEGs and differentially expressed eccDNA were intersected, and a set of 288 genes associated with drug resistance was then obtained, showing different expression levels in both mRNA and eccDNA (Fig. 5E).

Subsequently, GO functional enrichment analysis was performed on these 288 common DEGs. The results showed that these genes were predominantly involved in biological processes such as DNA-binding transcription factor binding and ethanolamine kinase activity (Fig. 5F). Furthermore, KEGG pathway enrichment analysis was also conducted, and several significantly enriched signaling pathways were found, such as the Thyroid hormone signaling pathway, Dopaminergic synapse, and Circadian entrainment (Fig. 5G). A PPI network was also constructed using the STRING database, which consisted of 94 nodes and 80 edges (Fig. 5H). The topological properties of the PPI network were then analyzed using the cytoHubba tool in Cytoscape software, and 3 potential biomarkers (MED1, MED24, and NMD3) were obtained (Fig. 5I). To further understand the molecular mechanisms of drug resistance, we performed the classical signaling pathway enrichment analysis of these 288 DEGs using the IPA software. The result demonstrated that the Synaptogenesis Signaling Pathway and Adipogenesis pathway were activated, while pathways such as Neuroprotective Role of THOP1 in Alzheimer's Disease, MSP-RON Signaling in Macrophages Pathway, and SNARE Signaling Pathway were identified as inhibited

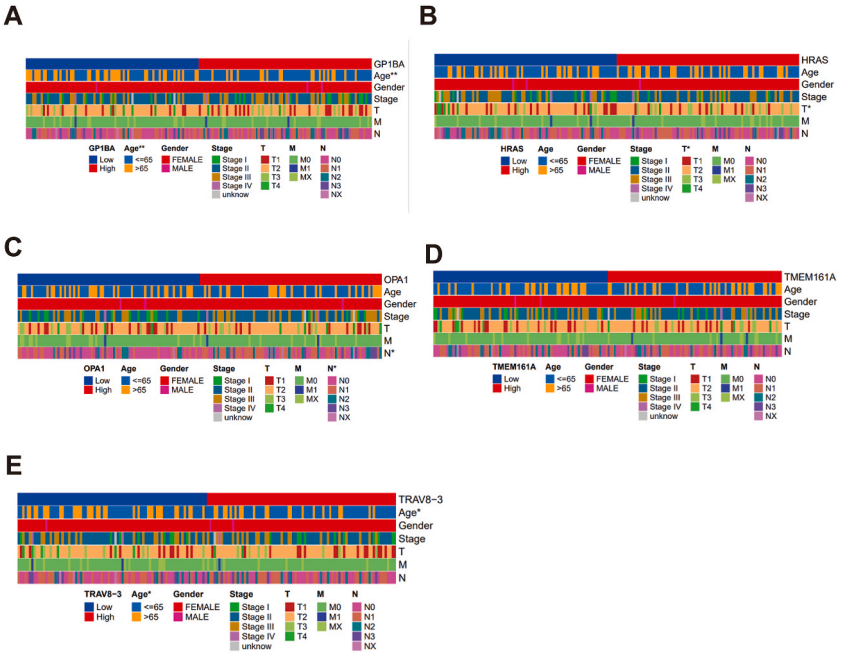

Fig. 4. Correlation analysis of the predictive model with clinical factors. (A–E) The bar chart of the correlation between every single gene and different clinical factors, as indicated in different colors, respectively.

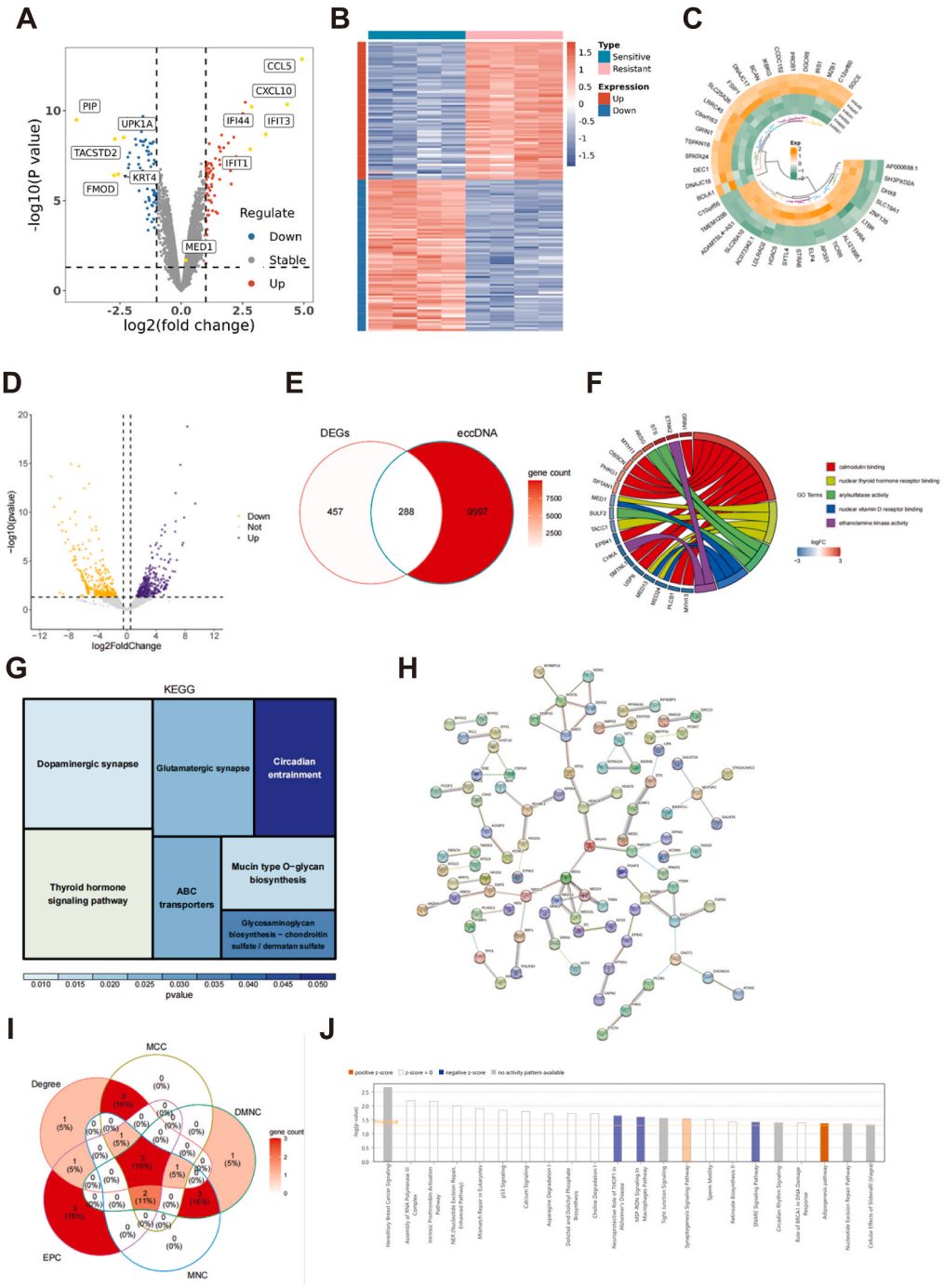

Fig. 5. Functional analysis of DEGs related to drug resistance. (A) The volcano plot of differentially expressed genes (DEGs) analyzed from the GEO dataset, where red represents upregulated genes in the Resistant samples compared to the Sensitive samples and blue represents downregulated genes. The gray dots indicate that these genes do not show significant differences. (B) The heatmap of DEGs, where red represents upregulated genes in the Resistant samples compared to the Sensitive samples and blue represents downregulated genes. The gray dots indicate that these genes do not show significant differences. (C) The heatmap of the common DEGs, with the color of each box representing the relative expression levels of the gene in the corresponding sample, green indicating low expression, and orange indicating high expression. (D) The volcano plot of the DEGs between two groups. Each point on the plot represents a gene. Yellow and purple points represent significant DEGs, with purple indicating upregulated differential expression and yellow indicating downregulated differential expression. Gray points represent genes without significant differences. (E) The Venn diagram of the common DEGs. (F) The chord diagram of the enrichment analysis results of GO terms, where the genes participating in the same GO terms are connected by colored links, and the magnitude of the variation is indicated by a color gradient mapping. (G) The KEGG pathway enrichment analysis. (H) The image of the PPI network. (I) The Venn diagram of selective key genes. (J) The bar chart of the classical signaling

pathways associated with DEGs. The size of each circle corresponds to the number of genes involved in that pathway. Orange circles indicate predicted activated pathways, blue circles represent predicted inhibited pathways, gray circles indicate pathways for which automatic scoring prediction is currently not available, and white circles represent pathways where there is currently insufficient evidence to predict activation or inhibition.

(Fig. 5J).

3.7. Analysis of differently expressed non-coding RNA

To further investigate the potential role of non-coding RNA in regulating drug resistance of HER2-positive breast cancer, we compared the expression levels of miRNA, lncRNA, and circRNA in SK-BR-3 cells and JIMT-1 cells. According to the results, 610 differently expressed miRNA (287 upregulated genes and 323 downregulated genes) (Fig. 6A), 22 differently expressed lncRNA (7 upregulated genes and 15 downregulated genes) (Fig. 6B), and 32 differently expressed circRNA (14 upregulated genes and 18 downregulated genes) (Fig. 6C) were identified. Next, key miRNA prediction analysis was conducted to predict miRNAs targeting the identified key genes using the miRWalk tool. Afterward, these predicted miRNAs were then intersected with the differentially expressed miRNAs, and a set of 57 miRNAs was obtained and denoted as key miRNAs (Fig. 6D). Subsequently, the target lncRNAs of these key miRNAs were predicted, and then the predicted lncRNAs were intersected with the differentially expressed lncRNAs. A crucial lncRNA (LINC00960) was finally obtained (Fig. 6E). Moreover, an mRNA-miRNA-lncRNA regulatory network was constructed using the retrieved data (Fig. 6F). Additionally, the corresponding circRNAs of key miRNAs were also predicted using the starbase database. After intersecting the predicted circRNAs with the differentially expressed circRNAs, 2 important circRNAs (hsa_circ_0001326 and hsa_circ_0001776) (Fig. 6G) were identified, as well as an mRNA-miRNA-circRNA regulatory network (Fig. 6H).

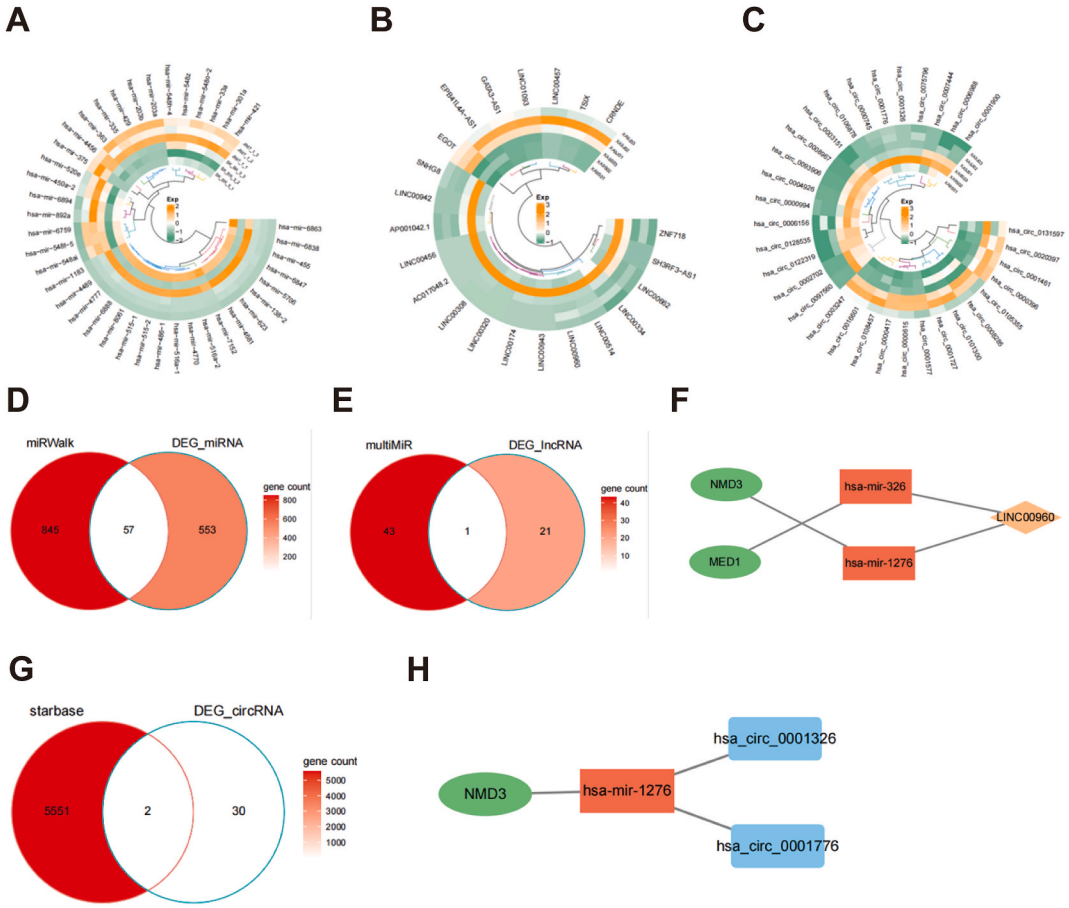

Fig. 6. Analysis of drug resistance-related non-coding RNA network. (A–C) The heatmap of differently expressed non-coding RNAs, including miRNA (A), lncRNAs (B), and circRNAs (C). (D and E) The Venn diagram showing the crucial miRNA (D) and lncRNA (E). (F) The regulatory network of mRNA-miRNA-lncRNA. (G) The Venn diagram showing the crucial circRNA. (H) The regulatory network of mRNA-miRNA-circRNA.

3.8. Validation of the selected 3 crucial genes

As shown before, 3 three crucial genes (MED1, MED24, and NMD3) mediating drug resistance of breast cancer were selected and obtained. These results were first validated using qPCR. The results showed that all 3 genes were markedly upregulated in the drug-resistant cell line JIMT-1 compared to those in SK-BR-3 (Fig. 7A). After integrating resistance gene selecting results from the HER2-positive breast cancer dataset (GEO), eccDNA sequencing data, and transcriptome sequencing data, one most significantly DEG, MED1, was finally retrieved. It was found that MED1 was the most significantly elevated in drug-resistance cells, which implied that MED1 may play a crucial role in regulating drug resistance of HER2-positive breast cancer (Fig. 7B and C).

3.9. Functional analysis of MED1 in drug resistance in breast cancer cells

For further validating our screening results, cell and animal experiments were performed to determine whether the MED1 gene was associated with drug resistance in HER2-positive breast cancer. A MED1 knockdown cell line (JIMT-1-KD) was established in the trastuzumab-resistant JIMT-1 cell line using shRNA; a MED1 overexpression cell line (SKBR3-OE) was constructed in the trastuzumab-sensitive SKBR3 cell line using lentiviral techniques. qPCR and Western blot verified their mRNA and protein levels (Fig. 8A and B).

Subsequently, the molecular mechanism by which MED1 participates in trastuzumab resistance was elucidated. In short, SKBR3-OE cells and their control counterparts were treated with AG825 (HER2 inhibitor) or MK-8353 (ERK1/2 inhibitor). Cell viability after trastuzumab treatment was assessed using the CCK-8 assay to investigate whether MED1 mediated trastuzumab resistance through the HER2/ERK1/2 pathway. The results revealed that MED1 overexpression promoted SKBR3 cell proliferation; however, both AG825 and MK-8353 significantly inhibited SKBR3 cell proliferation regardless of MED1 overexpression (Fig. 8C).

Additionally, the in vivo experiments were also conducted to verify the above results. Tumor formation was induced in nude mice using MED1 knockdown JIMT-1-KD cells, MED1 overexpression SKBR3-OE cells, and their respective control cells. After tumor formation, the mice were treated with trastuzumab. As indicated by the results, MED1 knockdown significantly inhibited tumor growth; the JIMT-1-si-MED1 + trastuzumab group showed notably lower tumor volume and weight than the JIMT-1 control group. Conversely, MED1 overexpression promoted tumor growth; the tumor volume and weight in the SKBR3 Virus-oe-MED1 + trastuzumab group were remarkably higher compared to that in the SKBR3 Virus-oe-NC group(Fig. 8D and E).

4. Discussion

The present study identified a novel 5 ErbB-related gene signature (TRAV8-3, TMEM161A, OPA1, HRAS, and GP1BA) for predicting the prognosis of HER2-positive breast cancer patients. Additionally, MED1, MED24, and NMD3 emerged as key genes potentially linked to chemoresistance. Among them, MED1 was the most significantly elevated in chemoresistant cells, making it an attractive candidate target for treating the resistance of breast tumor cells to therapy.

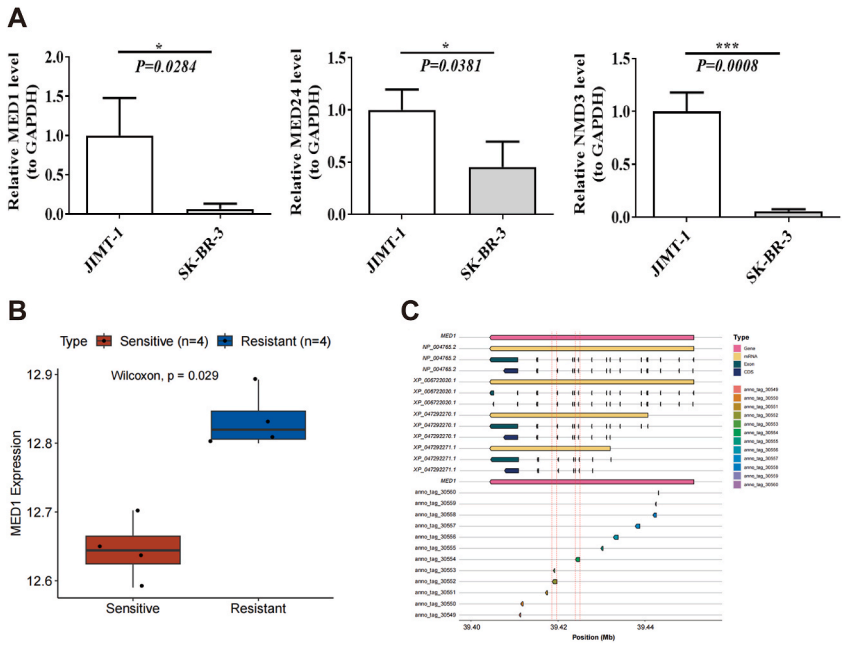

Fig. 7. Validation of the crucial DEGs. (A) qPCR analysis of the expression levels of MED1 (left), MED24 (middle), and NMD3 (right). (B) The expression level of MED1 in the Resistance and Sensitive groups from the GEO database. (C) The distribution region of the MED1 gene in the GH38 genome and eccDNA. *, $p < 0.05$; ***, $p < 0.001$.

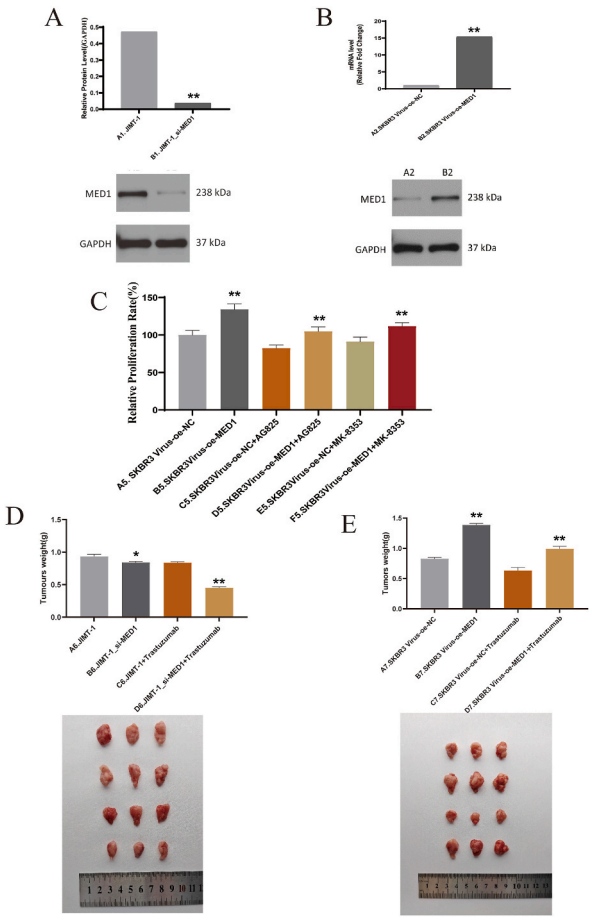

Fig. 8. Validation of MED1 in drug resistance mechanism. (A) qPCR and Western Blot analysis of MED1 mRNA and protein levels in JIMT-1 KD cells. (B) qPCR and Western Blot analysis of MED1 mRNA and protein levels in SKBR3-OE cells. (C) Cell viability assay (CCK-8) of different cell groups treated with trastuzumab. (D) Tumor weight measurement in nude mice implanted with MED1-deficient JIMT-1 KD cells and control cells. (E) Tumor weight measurement in nude mice implanted with MED1-overexpressing SKBR3-OE cells and control cells.*$P < 0.05$,**$P < 0.01$.

In this study, based on co-expression analysis, 1001 ErbB signaling pathway-related genes that might regulate HER2 activity in HER2-positive breast cancer patients were screened out. Following further enrichment analysis, these genes were found to predominantly participate in immune-related pathways and chemoresistance, which is consistent with the pathological process of HER2-positive breast cancer [27–29]. Subsequently, univariate and multivariate Cox regression analyses were performed and a prognostic model integrating ErbB signaling pathway-related genes (TRAV8-3, TMEM161A, OPA1, HRAS, and GP1BA) in HER2-positive breast cancer patients was established. The performance of this signature was validated in both TCGA cohorts, with ROC and Kaplan-Meier analysis results showing significant differences in survival between the low-risk and high-risk groups.

TRAV genes display complicated and diverse expression in patients with breast cancer, with certain TRAV genes showing preferential usage in the peripheral blood mononuclear cells (PBMCs) and tumor-in-filtrating lymphocytes (TILs). Especially, it has been evidenced that the frequencies of TRAV1.1 and TRAV22 exceed 30 % in TILs and those of TRAV1.1, TRAV9, and TRAV29 exceed 30 % in PBMCs; additionally, 5 of 8 patients with ER-positive breast cancer exhibit high expression of TRAV1.1 and TRAV32 [30]. However, there is currently very little empirical research concerning TRAV8-3. This study is the first to reveal its differential expression in breast cancer and the correlation of its enforced expression with the satisfactory prognosis of breast cancer patients. As has been evidenced previously, the epithelial protein TMEM161A is highly expressed in human lung cancer tissues and cross-reactive epitopes from Epstein-Barr virus and E. coli; $CD8^+$ T cells with the "S%DGMNTE'' motif cross-react with the TMEM161A tumor antigen, and recognition of the cross-reactive TMEM161A antigen on HLA-A*02 leads to target cell lysis by $CD8^+$ T cells with the "S%DGMNTE'' motif [31]. This indicated that TMEM161A may portend a dismal prognosis in lung cancer patients, and TMEM161A silencing may boost the anti-tumor immune responses. Additionally, a recent study has also demonstrated that TMEM161A is a potentially diagnostic biomarker for patients with osteonecrosis of the femoral head, which is a kind of disabling disease [32]. However, it remains elusive whether TMEM161A affects patient's survival. In this study, the survival analysis results indicated that low survival rates in HER2-positive breast cancer patients were closely associated with high TMEM161A expression. Consistently, a previous study has shown that upregulation of the mitochondrial fusion protein OPA1 can predict a poor prognosis in patients with breast cancer;

accordingly, OPA1 inhibition reduces breast cancer cell proliferation, migration, and invasion *in vitro* and in vivo via increasing expression of miRNAs of the 148/152 family [33]. OPA1 expression is increased in the resistant lung adenocarcinoma cells, and genetic or pharmacological inhibition of OPA1 restores the sensitivity to gefitinib in lung adenocarcinoma cells [34]. Additionally, HRAS, a common mutational oncogene, is prone to a mutation in various tumors, including breast cancer; HRAS is one of the hub targets of Syringin for breast cancer treatment, which is closely related to the survival and prognosis of breast cancer patients; the *in vitro* experiments also confirm that HRAS suppression contributes to the inhibiting effect of Syringin on breast cancer cell proliferation and migration [35]. These findings imply that HRAS upregulation may be associated with the poor prognosis of breast cancer patients, which differs from the present results. Moreover, previous evidence has demonstrated a significant association between the allelic level of the HRAS1 gene and breast cancer susceptibility [36]. Also, the downregulation of HRAS expression in head and neck squamous cell carcinoma cells leads to an increased erlotinib sensitivity *in vitro* and in vivo [37]. Hence, the accuracy of the results of this study regarding HRAS in predicting disease prognosis needs to be further investigated. In the study by Duan et al., GP1BA is enriched in the particle purification liquid chromatography (PPLC)-isolated blood plasma-derived extracellular vesicles from breast cancer patients who fail to achieve a pCR after neoadjuvant chemotherapy; moreover, their findings suggest that GP1BA may represent a predictor of chemoresistance in breast cancer [38]. Altogether, this evidence demonstrated that the ErbB-related genes-based molecular signature had an excellent performance for prognosis prediction in HER2-positive breast cancer.

Additionally, based on the GEO data, 3 key genes (MED1, MED24, and NMD3) were identified to be involved in the regulation of chemoresistance in HER2-positive breast cancer patients. After a series of further intersection analyses with eccDNA sequencing and transcriptome sequencing, MED1 was identified as a hub gene with its significant elevation in drug-resistant cells, indicating that it may play a crucial role in mediating drug resistance. Indeed, the MED1 subunit of the Mediator complex is a central transcriptional coactivator complex, which is capable of directly interacting with ER to mediate its functions [39]. MED1 is abundantly expressed in most human breast cancer cases and mediates breast cancer metastasis and treatment resistance [40]. MED1 co-amplifies with HER2 and MED1 silencing can sensitize breast cancer cells to HER2-mediated chemoresistance [41,42]. MED1 upregulation by leptin is partially mediated by HER2 and EGFR activation, and the leptin-Her2-EGFR-Med1 axis may be implicated in the poor response to tamoxifen in breast cancer patients [43]. MED24 is also a component of the Mediator complex; MED24 is highly expressed in various breast cancer cell lines, and MED24 downregulation attenuates tumor growth in breast cancer [44,45]. As a highly conserved protein in eukaryotes, NMD3 serves as an essential adaptor for the Crm1-dependent export of large ribosomal subunits from the nucleus [46, 47]. Emerging evidence has confirmed NMD3 to be the most promising differentially expressed target in chemoresistance development as its expression is reduced in MCF-7 breast cancer cells following doxorubicin treatment [48]. Taken together, the above findings and evidence indicated that MED1, MED24, and NMD3 proteins were crucial in resistance development; targeting these proteins will facilitate their usage in overcoming chemoresistance in breast cancer.

The activation of the synaptogenesis signaling pathway may influence cellular communication and signaling networks to potentially contribute to drug resistance in HER2-positive breast cancer, thereby enhancing tumor cell survival and proliferation. The GPCR involved in synaptogenesis, BAI1, has been identified as a key prognostic factor in predicting breast cancer metastasis [49]. Research has shown that neurons can form synapses with non-neuronal cancer cells, thus promoting brain metastasis in melanoma and breast cancer [50]. Cancer-associated adipocytes can secret various cytokines and growth factors to influence the tumor microenvironment. These adipocytes can promote cancer cell invasion, migration, and survival via mediating pathways (such as JAK/STAT3, and NF-κB) involved in drug resistance mechanisms [51]. Elevated IL-6 and TNF-α levels in the tumor microenvironment have been shown to be tightly linked to increased cancer stem cell populations and enhanced tumor aggressiveness, which contributes to resistance against therapies such as trastuzumab and lapatinib [52]. GnRH has antitumor effects, while the active metabolite GnRH-(1–5) produced by GnRH catalytic breakdown by THOP1 requires further investigation [53]. The MSP-RON pathway has been shown to suppress T cell activity and enable metastasis, which makes treatment further complicated and promote drug resistance [54,55]. The SNARE signaling pathway is crucial for vesicle fusion and neurotransmitter release, and its inhibition could disrupt cellular communication and vesicular transport, which is essential for maintaining cellular homeostasis; moreover, this disruption may contribute to drug resistance by affecting drug uptake and efflux mechanisms in cancer cells, making them less responsive to treatments [56].

MED1 was specifically focused in this study via conducting detailed *in vitro* and in vivo experiments. MED1 was knocked down in the trastuzumab-resistant JIMT-1 cell line (JIMT-1-KD) and overexpressed in the trastuzumab-sensitive SKBR3 cell line (SKBR3-OE) using shRNA. Our results demonstrated that MED1 knockdown significantly inhibited proliferation and increased trastuzumab sensitivity in JIMT-1 cells. Conversely, MED1 overexpression markedly promoted SKBR3 cell proliferation, even in the presence of trastuzumab. These effects were intrinsically linked to the HER2/ERK1/2 pathway, as evidenced by inhibitors of HER2 and ERK1/2 reducing cell proliferation irrespective of MED1 expression.

These findings were further validated through the in vivo studies. Tumor growth was notably reduced with MED1 knockdown and increased with MED1 overexpression in the presence of trastuzumab. This underscores the crucial role of MED1 in mediating trastuzumab resistance and its great potential as a therapeutic target.

5. Conclusion

In conclusion, this study successfully constructed a 5 ErbB-related gene signature that can predict the prognosis of HER2-positive breast cancer patients. Our results highlight that MED1 is a key player in trastuzumab resistance in HER2-positive breast cancer, suggesting that targeting MED1, along with HER2/ERK1/2 pathway inhibitors, could enhance treatment efficacy and overcome resistance.

Funding

This research did not receive any specific grant from funding agencies in the public, commercial, or not-for-profit sectors.

Data availability statement

The data that support the findings of this study are available from the corresponding author upon reasonable request.

Ethical statement

The authors are accountable for all aspects of the work in ensuring that questions related to the accuracy or integrity of any part of the work are appropriately investigated and resolved. The study was conducted following the Declaration of Helsinki (as revised in 2013). All animals were kept in a pathogen-free environment and fed ad libitum. All applicable institutional and governmental regulations concerning the ethical use of animals were followed. The study was approved by the Ethics Committee at The Second Affiliated Hospital of Air Force Medical University (No. K202010-04).

Consent for participate

Informed consent was obtained from all patients involved in the study.

Consent for publication

Not applicable.

CRediT authorship contribution statement

Lin Yang: Writing – original draft, Methodology, Formal analysis, Data curation, Conceptualization. **Songhao Chen:** Formal analysis, Data curation. **Meixue Wang:** Methodology, Data curation. **Shujia Peng:** Methodology, Data curation. **Huadong Zhao:** Supervision. **Ping Yang:** Writing – review & editing, Formal analysis. **Guoqiang Bao:** Writing – review & editing, Supervision. **Xianli He:** Writing – review & editing, Formal analysis.

Declaration of competing interest

The authors declare that they have no known competing financial interests or personal relationships that could have appeared to influence the work reported in this paper.

Acknowledgment

We would like to acknowledge the reviewers for their helpful comments on this paper.

Appendix A. Supplementary data

Supplementary data to this article can be found online at https://doi.org/10.1016/j.heliyon.2024.e38221.

References

[1] S. Loibl, et al., Breast cancer, Lancet 397 (10286) (2021) 1750–1769.
[2] M.L. Uribe, I. Marrocco, Y. Yarden, EGFR in cancer: signaling mechanisms, drugs, and acquired resistance, Cancers 13 (11) (2021).
[3] S. Loibl, L. Gianni, HER2-positive breast cancer, Lancet 389 (10087) (2017) 2415–2429.
[4] G.M. Choong, G.D. Cullen, C.C. O'Sullivan, Evolving standards of care and new challenges in the management of HER2-positive breast cancer, CA Cancer J Clin 70 (5) (2020) 355–374.
[5] Z. Sirhan, A. Thyagarajan, R.P. Sahu, The efficacy of tucatinib-based therapeutic approaches for HER2-positive breast cancer, Mil Med Res 9 (1) (2022) 39.
[6] J.Z. Drago, et al., Beyond HER2: targeting the ErbB receptor family in breast cancer, Cancer Treat Rev. 109 (2022) 102436.
[7] A. Pellat, J. Vaquero, L. Fouassier, Role of ErbB/HER family of receptor tyrosine kinases in cholangiocyte biology, Hepatology 67 (2) (2018) 762–773.
[8] S. Kumagai, S. Koyama, H. Nishikawa, Antitumour immunity regulated by aberrant ERBB family signalling, Nat. Rev. Cancer 21 (3) (2021) 181–197.
[9] F. Ge, Y. Du, Y. He, Direct observation of endocytosis dynamics of anti-ErbB modified single nanocargoes, ACS Nano 16 (4) (2022) 5325–5334.
[10] J. Foley, et al., EGFR signaling in breast cancer: bad to the bone, Semin. Cell Dev. Biol. 21 (9) (2010) 951–960.
[11] M.L. Hagan, et al., Upregulation of the EGFR/MEK1/MAPK1/2 signaling axis as a mechanism of resistance to antiestrogen-induced BimEL dependent apoptosis in ER(+) breast cancer cells, Int. J. Oncol. 62 (2) (2023).
[12] S. Lev, Targeted therapy and drug resistance in triple-negative breast cancer: the EGFR axis, Biochem. Soc. Trans. 48 (2) (2020) 657–665.
[13] I. Shin, HER2 signaling in breast cancer, Adv. Exp. Med. Biol. 1187 (2021) 53–79.
[14] R. Martinello, et al., Investigational ErbB-2 tyrosine kinase inhibitors for the treatment of breast cancer, Expert Opin Investig Drugs 25 (4) (2016) 393–403.

[15] F. Xing, et al., CMTM6 overexpression confers trastuzumab resistance in HER2-positive breast cancer, Mol. Cancer 22 (1) (2023) 6.
[16] H.J. Choi, et al., Role of RBP2-induced ER and igf1r-ErbB signaling in tamoxifen resistance in breast cancer, J Natl Cancer Inst 110 (4) (2018).
[17] J. Zhou, S. Zhang, M. Luo, LncRNA PCAT7 promotes the malignant progression of breast cancer by regulating ErbB/PI3K/Akt pathway, Future Oncol. 17 (6) (2021) 701–710.
[18] J.N. Weinstein, et al., The cancer genome Atlas pan-cancer analysis project, Nat. Genet. 45 (10) (2013) 1113–1120.
[19] R. Edgar, M. Domrachev, A.E. Lash, Gene Expression Omnibus: NCBI gene expression and hybridization array data repository, Nucleic Acids Res. 30 (1) (2002) 207–210.
[20] M. Kanehisa, et al., KEGG: new perspectives on genomes, pathways, diseases and drugs, Nucleic Acids Res. 45 (D1) (2017) D353–d361.
[21] G. Yu, et al., clusterProfiler: an R package for comparing biological themes among gene clusters, OMICS 16 (5) (2012) 284–287.
[22] A. Krämer, et al., Causal analysis approaches in ingenuity pathway analysis, Bioinformatics 30 (4) (2014) 523–530.
[23] D. Szklarczyk, et al., STRING v11: protein-protein association networks with increased coverage, supporting functional discovery in genome-wide experimental datasets, Nucleic Acids Res. 47 (D1) (2019) D607–d613.
[24] P. Shannon, et al., Cytoscape: a software environment for integrated models of biomolecular interaction networks, Genome Res. 13 (11) (2003) 2498–2504.
[25] K.J. Livak, T.D. Schmittgen, Analysis of relative gene expression data using real-time quantitative PCR and the 2(-Delta Delta C(T)) Method, Methods 25 (4) (2001) 402–408.
[26] N. Simon, et al., Regularization paths for cox's proportional hazards model via coordinate descent, J Stat Softw 39 (5) (2011) 1–13.
[27] H.L. Chang, et al., Antibody-drug conjugates in breast cancer: overcoming resistance and boosting immune response, J. Clin. Invest. 133 (18) (2023).
[28] L. Yang, et al., A recombinant human protein targeting HER2 overcomes drug resistance in HER2-positive breast cancer, Sci. Transl. Med. 11 (476) (2019).
[29] M. Luque, et al., Tumor-infiltrating lymphocytes and immune response in HER2-positive breast cancer, Cancers 14 (24) (2022).
[30] X.Y. He, et al., TRAV gene expression in PBMCs and TILs in patients with breast cancer analyzed by a DNA melting curve (FQ-PCR) technique for TCR α chain CDR3 spectratyping, Neoplasma 59 (6) (2012) 693–699.
[31] S.H. Chiou, et al., Global analysis of shared T cell specificities in human non-small cell lung cancer enables HLA inference and antigen discovery, Immunity 54 (3) (2021) 586–602.e8.
[32] Z. Chen, et al., Comprehensive analysis of femoral head necrosis based on machine learning and bioinformatics analysis, Medicine (Baltim.) 102 (23) (2023) e33963.
[33] M. Zamberlan, et al., Inhibition of the mitochondrial protein Opa1 curtails breast cancer growth, J. Exp. Clin. Cancer Res. 41 (1) (2022) 95.
[34] M. Noguchi, et al., Inhibition of the mitochondria-shaping protein Opa1 restores sensitivity to Gefitinib in a lung adenocarcinomaresistant cell line, Cell Death Dis. 14 (4) (2023) 241.
[35] F. Wang, et al., Syringin exerts anti-breast cancer effects through PI3K-AKT and EGFR-RAS-RAF pathways, J. Transl. Med. 20 (1) (2022) 310.
[36] L.N. Al-Eitan, B.H. Al-Ahmad, F.A. Almomani, The association of IL-1 and HRAS gene polymorphisms with breast cancer susceptibility in a Jordanian population of arab descent: a genotype-phenotype study, Cancers 12 (2) (2020).
[37] J.H. Hah, et al., HRAS mutations and resistance to the epidermal growth factor receptor tyrosine kinase inhibitor erlotinib in head and neck squamous cell carcinoma cells, Head Neck 36 (11) (2014) 1547–1554.
[38] F.A. Alvarez, et al., Blood plasma derived extracellular vesicles (BEVs): particle purification liquid chromatography (PPLC) and proteomic analysis reveals BEVs as a potential minimally invasive tool for predicting response to breast cancer treatment, Breast Cancer Res. Treat. 196 (2) (2022) 423–437.
[39] D. Zhang, et al., Arginine and glutamate-rich 1 (ARGLU1) interacts with mediator subunit 1 (MED1) and is required for estrogen receptor-mediated gene transcription and breast cancer cell growth, J. Biol. Chem. 286 (20) (2011) 17746–17754.
[40] M. Leonard, X. Zhang, Estrogen receptor coactivator Mediator Subunit 1 (MED1) as a tissue-specific therapeutic target in breast cancer, J. Zhejiang Univ. - Sci. B 20 (5) (2019) 381–390.
[41] J. Cui, et al., Cross-talk between HER2 and MED1 regulates tamoxifen resistance of human breast cancer cells, Cancer Res. 72 (21) (2012) 5625–5634.
[42] Y. Yang, et al., Functional cooperation between co-amplified genes promotes aggressive phenotypes of HER2-positive breast cancer, Cell Rep. 34 (10) (2021) 108822.
[43] A. Nagalingam, et al., Hyperleptinemia in obese state renders luminal breast cancers refractory to tamoxifen by coordinating a crosstalk between Med1, miR205 and ErbB, NPJ Breast Cancer 7 (1) (2021) 105.
[44] K. Kämpjärvi, et al., Somatic MED12 mutations in prostate cancer and uterine leiomyomas promote tumorigenesis through distinct mechanisms, Prostate 76 (1) (2016) 22–31.
[45] N. Hasegawa, et al., Mediator subunits MED1 and MED24 cooperatively contribute to pubertal mammary gland development and growth of breast carcinoma cells, Mol. Cell Biol. 32 (8) (2012) 1483–1495.
[46] C. Ma, et al., Structural snapshot of cytoplasmic pre-60S ribosomal particles bound by Nmd3, Lsg1, Tif6 and Reh1, Nat. Struct. Mol. Biol. 24 (3) (2017) 214–220.
[47] M. Oeffinger, Joining the interface: a site for Nmd3 association on 60S ribosome subunits, J. Cell Biol. 189 (7) (2010) 1071–1073.
[48] A.K. Sommer, et al., A proteomic analysis of chemoresistance development via sequential treatment with doxorubicin reveals novel players in MCF-7 breast cancer cells, Int. J. Mol. Med. 42 (4) (2018) 1987–1997.
[49] W.H. Meisen, et al., Changes in Bai1 and nestin expression are prognostic indicators for survival and metastases in breast cancer and provide opportunities for dual targeted therapies, Mol. Cancer Therapeut. 14 (1) (2015) 307–314.
[50] V. Venkataramani, et al., Direct excitatory synapses between neurons and tumor cells drive brain metastatic seeding of breast cancer and melanoma, bioRxiv (2024) 2024, 01.08.574608.
[51] Q. Wu, et al., Cancer-associated adipocytes: key players in breast cancer progression, J. Hematol. Oncol. 12 (1) (2019) 95.
[52] Y.-C. Wang, et al., Different mechanisms for resistance to trastuzumab versus lapatinib in HER2- positive breast cancers - role of estrogen receptor and HER2 reactivation, Breast Cancer Res. 13 (6) (2011) R121.
[53] G. Mezo, et al., New derivatives of GnRH as potential anticancer therapeutic agents, Curr. Med. Chem. 15 (23) (2008) 2366–2379.
[54] D. Sanjeev, et al., A network map of macrophage-stimulating protein (MSP) signaling, Journal of Cell Communication and Signaling 17 (3) (2023) 1113–1120.
[55] H. Eyob, Breast Cancer Metastasis and the Immune Response: MSP/Ron Signaling Suppresses CD8 T Cell Activity and Enables Metastasis, Department of Oncological Sciences, University of Utah, 2013.
[56] H. Liu, et al., SNARE proteins: core engines of membrane fusion in cancer, Biochim. Biophys. Acta Rev. Canc (2024) 189148.